

Nonlinear metal–dielectric nanoantennas for light switching and routing

This article has been downloaded from IOPscience. Please scroll down to see the full text article.

2012 New J. Phys. 14 093005

(<http://iopscience.iop.org/1367-2630/14/9/093005>)

View [the table of contents for this issue](#), or go to the [journal homepage](#) for more

Download details:

IP Address: 130.56.107.38

The article was downloaded on 11/04/2013 at 08:47

Please note that [terms and conditions apply](#).

Nonlinear metal–dielectric nanoantennas for light switching and routing

R E Noskov^{1,3}, A E Krasnok¹ and Yu S Kivshar^{1,2}

¹ National Research University of Information Technologies, Mechanics and Optics (ITMO), St Petersburg 197101, Russia

² Nonlinear Physics Centre, Research School of Physics and Engineering, Australian National University, Canberra, ACT 0200, Australia
E-mail: nanometa@gmail.com

New Journal of Physics **14** (2012) 093005 (10pp)


Received 11 May 2012

Published 4 September 2012

Online at <http://www.njp.org/>

doi:10.1088/1367-2630/14/9/093005

Abstract. We introduce a novel hybrid metal–dielectric nanoantenna composed of dielectric (crystalline silicon) and metal (silver) nanoparticles. In such a nanoantenna, the phase shift between the dipole moments of the nanoparticles, caused by differences in the polarizabilities, allows for directional light scattering; while the nonlinearity of the metal nanoparticle helps to control the radiation direction. We show that the radiation pattern of this nanoantenna can be switched between the forward and backward directions by varying only the light intensity around the level of 6 MW cm^{-2} , with a characteristic switching time of 40 fs.

 Online supplementary data available from stacks.iop.org/NJP/14/093005/mmedia

³ Author to whom any correspondence should be addressed.



Content from this work may be used under the terms of the [Creative Commons Attribution-NonCommercial-ShareAlike 3.0 licence](http://creativecommons.org/licenses/by-nc-sa/3.0/). Any further distribution of this work must maintain attribution to the author(s) and the title of the work, journal citation and DOI.

Contents

1. Introduction	2
2. Model	2
3. Results and discussions	5
4. Conclusions	8
Acknowledgments	9
References	9

1. Introduction

The study of optical nanoantennas has become the subject of intensive research [1, 2]. Nanoantennas hold the promise of subwavelength manipulation and the control of optical radiation for solar cells and sensing [3]. In the majority of applications, a crucial factor is the control over the nanoantenna's radiation pattern and its tunability. Spectral tunability and variable directionality have been proposed for bimetallic antennas [4, 5], the Yagi–Uda architectures [6, 7], mechanically reconfigurable Au nanodimers [8], high-permittivity dielectric nanoparticles [9, 10] and for nanoparticle chains [11]. In addition, several suggestions employed the concept of plasmonic nanoantennas with a nonlinear load where the spectral tunability is achieved by varying the pumping energy [12–16].

In this paper, we suggest and study theoretically a novel type of metal–dielectric nanoantenna structure composed of a pair of dielectric (e.g. crystalline silicon) and metal (e.g. silver) nanoparticles. The combination of a high-permittivity dielectric and metallic nanoparticles makes it possible to achieve directional light scattering, whereas the nonlinear response of a metal nanoparticle helps to control the radiation direction of the nanoantenna. As a result, for such a structure we can realize efficient dynamical control over the scattering pattern by varying the external field intensity. An estimated switching time of 40 fs, along with the relatively low required intensities of about 6 MW cm^{-2} , opens a promising perspective for using nonlinear metal–dielectric nanoantennas in logical and switching devices.

2. Model

We consider a pair of spherical silicon and silver nanoparticles embedded into a SiO_2 host medium with permittivity ϵ_h , excited by a plane wave, as shown in figure 1. We assume that the radii of the metallic and dielectric nanoparticles and the center-to-center distance are $R_{\text{Ag}} = 15 \text{ nm}$, $R_{\text{Si}} = 30 \text{ nm}$ and $d = 80 \text{ nm}$, respectively. As the gap between particle surfaces $s = d - R_{\text{Si}} - R_{\text{Ag}}$ exceeds $\min\{R_{\text{Ag}}; R_{\text{Si}}\}$, we can employ the point dipole approximation [17–19]. In the optical spectral range, a linear part of a silver dielectric constant can be written in a generalized Drude form $\epsilon_{\text{Ag}}^{\text{L}} = \epsilon_{\infty} - \omega_p^2 / [\omega(\omega + i\nu)]$, where $\epsilon_{\infty} = 4.96$, $\hbar\omega_p = 9.54 \text{ eV}$, $\hbar\nu = 0.055 \text{ eV}$ [20] ($\exp(-i\omega t)$ time dependence is assumed); whereas dispersion of SiO_2 can be neglected since $\epsilon_h \simeq 2.2$ for photon energies 2.8–3.2 eV [21]. In this range, the permittivity of silicon ϵ_{Si} changes from 23 to 36 [21] approximately; we take this experimental data into account but it will be shown below that the impact of silicon dispersion on the system dynamics is insignificant as

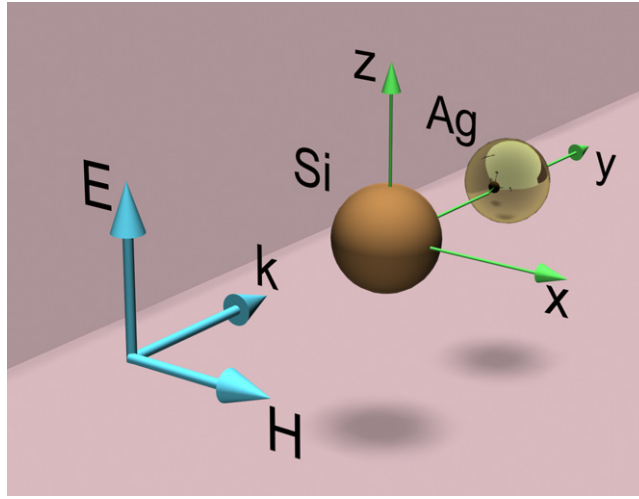


Figure 1. Schematic view of a dimer metal–dielectric nanoantenna.

well. The nonlinear dielectric constant of silver is $\varepsilon_{\text{Ag}}^{\text{NL}} = \varepsilon_{\text{Ag}}^{\text{L}} + \chi^{(3)} |\mathbf{E}^{(\text{in})}|^2$, where $\mathbf{E}^{(\text{in})}$ is the local field inside the particle. We keep only the cubic susceptibility due to the spherical symmetry of the silver particle. In general, the value of the cubic susceptibility for metallic nanoparticles depends on the type of metal, particle size, external pulse duration and frequency, as well as some other factors [22]. However, the analytical quantum model, developed in [23, 24] and confirmed with numerical simulations [25] and experimental data [26, 27], showed that silver nanoparticles with a 15 nm radius and driven at a frequency close to the frequency of the surface plasmon resonance, possess a remarkably high and purely real cubic susceptibility $\chi^{(3)} \simeq 6 \times 10^{-9}$ esu, in comparison to which the cubic nonlinearity of both Si and SiO_2 are negligibly weak ($\sim 10^{-12}$ esu [28] and $\sim 10^{-15}$ esu [29], respectively).

We have chosen silver due to its relatively low loss as well as its high nonlinear susceptibility, while the quite high permittivity of silicon leads to a pretty large extinction cross-section of the Si nanoparticle, which makes directional scattering from an asymmetric dimer possible. Fused silica was taken as the host matrix in order to cause a red shift of the surface plasmon resonance frequency of the Ag nanoparticle, and to obtain it in blue light where silicon shows relatively small losses. In addition, SiO_2 possesses a good enough optical transparency [21] to maintain the strong laser powers needed for the observation of nonlinear switching.

First, we start from the Fourier transforms of the particle electric-dipole moments

$$\begin{aligned} p_{\text{Si},z} &= \alpha_{\text{Si}} (E_z^{(\text{ex})} + A p_{\text{Ag},z}), \\ p_{\text{Ag},z} &= \alpha_{\text{Ag}} (E_z^{(\text{ex})} \exp(ikd) + A p_{\text{Si},z}), \end{aligned} \quad (1)$$

where $A = [\exp(ikd)/(\varepsilon_{\text{h}}d)][k^2 - (1/d^2) + (ik/d)]$ describes the dipole–dipole interaction between particles, $k = \omega/c\sqrt{\varepsilon_{\text{h}}}$ is the wavenumber, c is the speed of light, $E_z^{(\text{ex})}$ is the amplitude of the plane wave,

$$\alpha_{\text{Ag}} = \varepsilon_{\text{h}} \left\{ \frac{\varepsilon_{\text{Ag}}^{\text{NL}}(\omega) + 2\varepsilon_{\text{h}}}{R_{\text{Ag}}^3 [\varepsilon_{\text{Ag}}^{\text{NL}}(\omega) - \varepsilon_{\text{h}}]} + i \frac{2}{3} k^3 \right\}^{-1}$$

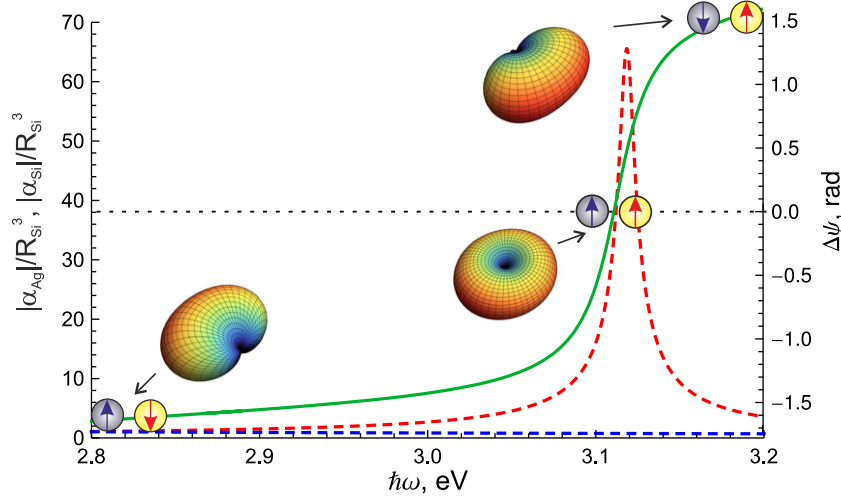


Figure 2. The full green line denotes the relative phase shift between the dipole moments of nanoparticles, while the dashed lines show the polarizability modulus of silver (red) and silicon (blue) nanoparticles, normalized to R_{Si}^3 versus the frequency. The red and blue arrows indicate the orientation of the dipole moments induced in the particles at different frequencies. Insets show the scattering patterns of a nanodimer when: (i) $\hbar\omega = 2.8 \text{ eV}$ —the system scatters light in the backward direction; (ii) $\hbar\omega = 3.14 \text{ eV}$ —the scattering pattern is omnidirectional; (iii) $\hbar\omega = 3.2 \text{ eV}$ —the system scatters light in the forward direction.

and $\alpha_{\text{Si}} = 3ia_1/(2k^3)$ are the polarizabilities of silver and silicon particles, and a_1 is the electric-dipole Mie scattering coefficient [30]. The small size of the silver nanoparticle allows us to use a quasistatic expression for α_{Ag} with the radiation damping correction [31]. On the other hand, the local field inside a 60 nm silicon particle with a relatively large permittivity cannot be considered as purely homogenous. That is why we define α_{Si} through the electric-dipole Mie scattering coefficient.

To illustrate how to achieve the directional scattering pattern from an asymmetric dimer, we analyze the scattering intensity of two dipoles, which is given by

$$U(\phi, \theta) = \frac{ck^4}{8\pi\epsilon_{\text{h}}^{3/2}} \sin^2\theta \left[|p_{\text{Si},z}|^2 + |p_{\text{Ag},z}|^2 + 2|p_{\text{Si},z}||p_{\text{Ag},z}| \cos(\Delta\Psi + kd \sin\theta \sin\phi) \right],$$

where ϕ and θ are the spherical azimuthal and polar angles, respectively, and $\Delta\Psi$ denotes an internal phase shift between the two dipoles. $\Delta\Psi$ is determined by the complex particle polarizabilities and therefore varies with the size, shape and material composition of the particles. The first two terms in this expression describe the individual dipole contributions, while the latter is responsible for the interference between particle fields. Clearly, directional scattering can be obtained when $\Delta\Psi$ sufficiently differs from zero. In the linear limit $\Delta\Psi$ can be tuned in a wide range by a variation in the frequency, since the silver particle experiences the strong surface plasmon resonance at $\hbar\omega_0 = \hbar\omega_p/\sqrt{\epsilon_{\infty} + 2\epsilon_{\text{h}}} = 3.14 \text{ eV}$; whereas α_{Si} is almost frequency independent, as shown in figure 2. Similar to other nanoparticle systems with broken symmetry [4, 5, 9, 10], one may see a switching of the dimer scattering pattern during the growth of ω .

3. Results and discussions

Next, we study the nonlinear dynamics of the dimer by employing the dispersion relation method [32, 33] that allows us to derive a system of coupled equations for the slowly varying amplitudes of the particle dipole moments. This approach is based on the assumption that in the system there exist small and large time scales, which, in our case, is fulfilled automatically because the silver particle acts as a resonantly excited oscillator with a slow (in comparison with the light period) inertial response; whereas the almost frequency independent α_{Si} allows us to treat the silicon particle response as instantaneous. We rewrite equation (1) in the form

$$\begin{aligned} p_{\text{Si},z} &= \alpha_{\text{Si}}(E_z^{(\text{ex})} + Ap_{\text{Ag},z}), \\ \alpha_{\text{Ag}}^{-1} p_{\text{Ag},z} &= E_z^{(\text{ex})} \exp(ikd) + Ap_{\text{Si},z}. \end{aligned} \quad (2)$$

Assuming that $\chi^{(3)}|\mathbf{E}^{(\text{in})}|^2 \ll 1$ and $\nu/\omega_0 \ll 1$, we decompose $\alpha_{\text{Ag}}^{-1}(\omega)$ in the vicinity of ω_0 and keep the first-order terms for the derivatives describing the (actually small) broadening of the silver particle polarization spectrum,

$$\alpha_{\text{Ag}}^{-1} \approx \alpha_{\text{Ag}}^{-1}(\omega_0) + \left. \frac{d\alpha_{\text{Ag}}^{-1}}{d\omega} \right|_{\omega=\omega_0} \left(\Delta\omega + i \frac{d}{dt} \right), \quad (3)$$

where $\Delta\omega$ is the frequency shift from the resonant value. Taking into account the instantaneous response of the Si nanoparticle and the relatively low strength of the dipole–dipole interaction [$(R_{\text{Si,Ag}}/d)^3 \ll 1$], we set $\alpha_{\text{Si}} = \alpha_{\text{Si}}(\omega_0) = \alpha_{\text{Si}}^0$ and $A = A(\omega_0) = A_0$. Having expressed $\mathbf{E}^{(\text{in})}$ via $\mathbf{p}_{\text{Ag},z}$, we substitute equation (3) into equation (2) and obtain the equations

$$\begin{aligned} P_{\text{Si}} &= \alpha_{\text{Si}}^0 [E + A_0 P_{\text{Ag}}], \\ i \frac{dP_{\text{Ag}}}{d\tau} + (i\gamma + \Omega + |P_{\text{Ag}}|^2 + \delta\Omega) P_{\text{Ag}} &= E [\exp(ik_0d) + \alpha_{\text{Si}}^0 A_0], \end{aligned} \quad (4)$$

where $\delta\Omega = [3\varepsilon_{\text{h}}^2 R_{\text{Ag}}^3][2(\varepsilon_{\infty} + 2\varepsilon_{\text{h}})]^{-1} \alpha_{\text{Si}}^0 A_0^2$ is the resonant frequency shift from ω_0 caused by the dipole–dipole interaction, $P_{\text{Si,Ag}} = p_{(\text{Si,Ag}),z} \sqrt{\chi^{(3)}} (\sqrt{2(\varepsilon_{\infty} + 2\varepsilon_{\text{h}})} \varepsilon_{\text{h}} a^3)^{-1}$ and $E = -3\varepsilon_{\text{h}} \sqrt{\chi^{(3)}} E_z^{(\text{ex})} [8(\varepsilon_{\infty} + 2\varepsilon_{\text{h}})^3]^{-1/2}$ are slowly varying dimensionless amplitudes of the particle's dipole moments and the external electric field, respectively, $\gamma = \nu/(2\omega_0) + (k_0 a)^3 \varepsilon_{\text{h}} (\varepsilon_{\infty} + 2\varepsilon_{\text{h}})^{-1}$ is in charge of the thermal and radiation losses of the Ag particle, $k_0 = \omega_0/c\sqrt{\varepsilon_{\text{h}}}$, $\Omega = (\omega - \omega_0)/\omega_0$ and $\tau = \omega_0 t$. Equation (4) describes the temporal nonlinear dynamics of a hybrid Si–Ag dimer driven by the external plane wave with a frequency of $\omega \sim \omega_0$.

Next, we consider the stationary solution of equation (4), which can be written as follows:

$$\begin{aligned} P_{\text{Si}} &= \alpha_{\text{Si}}^0 [E + A_0 P_{\text{Ag}}], \\ (i\gamma + \Omega + |P_{\text{Ag}}|^2 + \delta\Omega) P_{\text{Ag}} &= E [\exp(ik_0d) + \alpha_{\text{Si}}^0 A_0]. \end{aligned} \quad (5)$$

When $\Omega < -\text{Re } \delta\Omega - \sqrt{3}(\gamma - \text{Im } \delta\Omega)$, the particle polarizations P_{Ag} and P_{Si} become three-valued functions of Ω with two stable (lower and upper) and one unstable (middle) branches, as shown in figure 3(a). As a consequence, bistability, in this case, also appears in the frequency dependency of the nanoantenna front-to-back ratio (see figure 3(b)). One may see a significant contrast in the scattering patterns corresponding to the different stable branches.

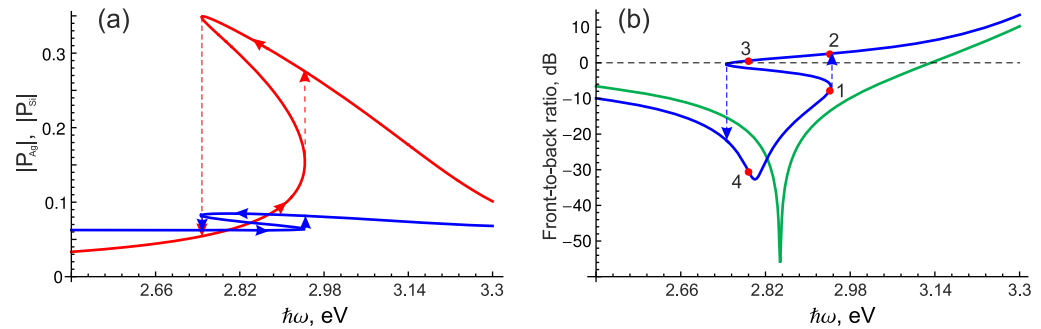


Figure 3. Frequency dependencies of (a) $|P_{Ag}|$ (red), $|P_{Si}|$ (blue) and (b) back-to-front ratio at the external intensity of 5.8 MW cm^{-2} ($E = 7.1 \times 10^{-3}$). In (b) green and blue curves correspond to linear and nonlinear cases, respectively. The middle branches inside the bistability loops correspond to the unstable solutions. Arrows show the transitions between the stable branches. Transitions between the stationary states marked by red dots at $\hbar\omega = 2.94 \text{ eV}$ ($\Omega = -0.062$) and $\hbar\omega = 2.8 \text{ eV}$ ($\Omega = -0.11$) were studied by numerical simulations of equation (4).

Being in the upper branch, the dimer scatters light predominantly in the forward direction or omnidirectionally, whereas the lower branch shows pronounced backscattering. Thus, having fixed ω close to one of the thresholds of the bistability region, one can switch the system's scattering pattern by varying the external field intensity.

To illustrate the dynamical control of the nanoantenna radiation, we solve equation (4) numerically at $\hbar\omega = 2.94 \text{ eV}$ ($\Omega = -0.062$) and $\hbar\omega = 2.8 \text{ eV}$ ($\Omega = -0.11$) and zero initial conditions. The stable system states generated by these frequencies are marked in figure 3(b) by red dots, and the scattering patterns, corresponding to $\hbar\omega = 2.94$ and 2.8 eV , are shown in figures 4(a)–(d). To initiate the system's transition from state 1 to state 2, we assume that the intensity of the pump pulse varies, slowly growing to the saturation level 5.8 MW cm^{-2} . Then, when the system is in state 1, the Gaussian signal pulse appears, provoking the system's transition to state 2, as shown in figure 5(a).

To initiate the transition between states 3 and 4, we at first deliver the system to state 3 by adding the Gaussian pulse centered around 20 fs to the pump pulse, slowly increasing again to the level 5.8 MW cm^{-2} , because state 3 belongs to the upper branch of the bistability loop. Then, at $t \sim 170 \text{ fs}$ a signal pulse, being out of phase with a pump pulse, results in switching, as shown in figure 5(b).

In both cases the characteristic switching time is 40 fs, and the saturation intensity level is 5.8 MW cm^{-2} . However, such high illuminating powers can lead to thermal damage of the dimer. To estimate the maximal pulse duration, we rely on the results of previous studies on the ablation thresholds for silver particles [34] and silicon films [35] providing values about 3.96 and 0.4 J cm^{-2} , respectively, for the picosecond regime of illumination. Taking into account the amplification of the electric field inside the Ag nanoparticle, due to surface plasmon resonance and the required intensity of 6 MW cm^{-2} , we come to the maximal pulse durations of 1 and 36 ns corresponding to the Ag and the Si particles, which are much longer than the characteristic switching time. Thus, the proposed metal–dielectric nanoantenna is fully suitable

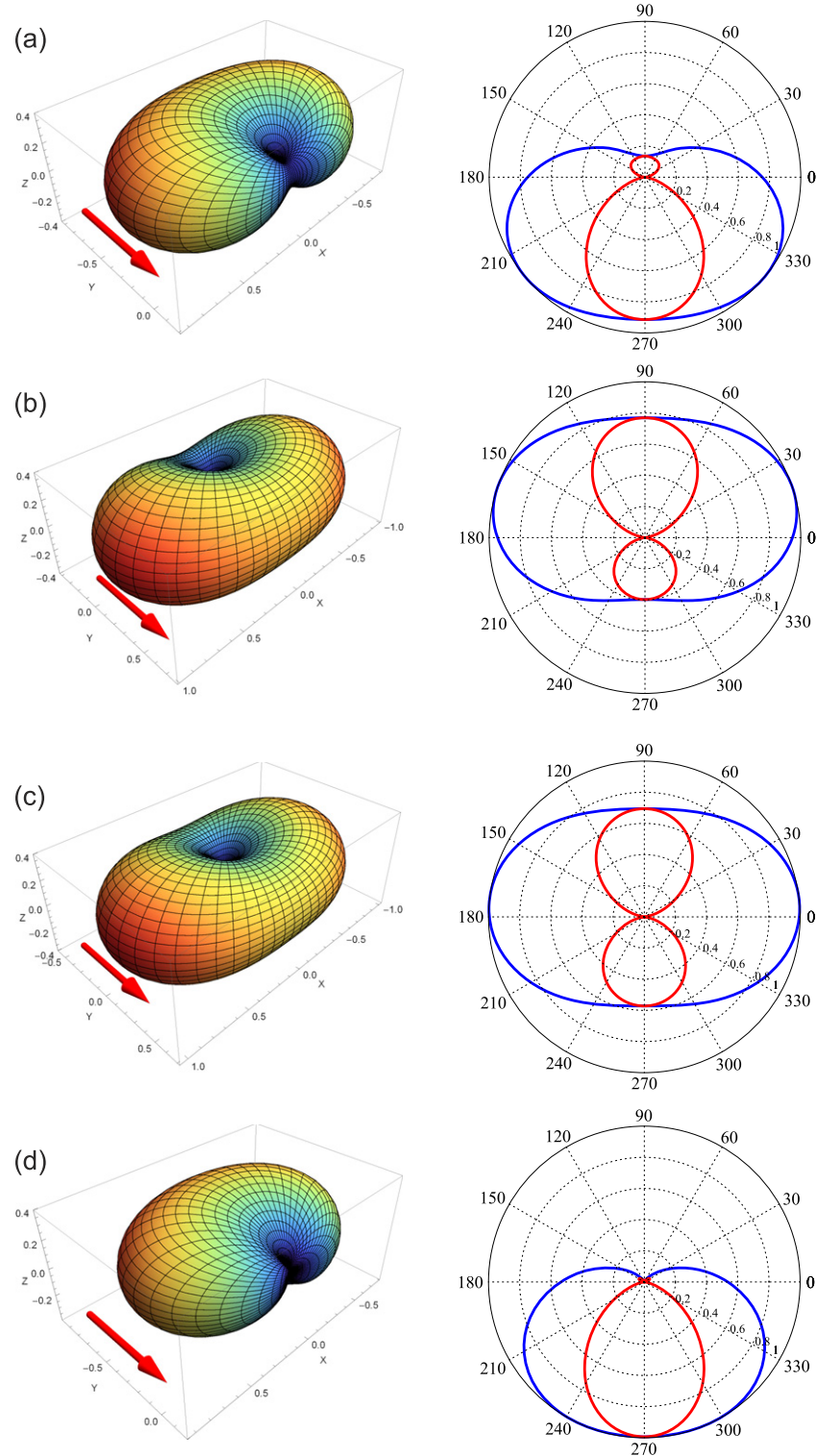


Figure 4. Normalized scattering patterns of the metal–dielectric nanoantenna for the stationary states denoted by red dots 1 (a), 2 (b), 3 (c) and 4 (d) in figure 3. Red and blue curves indicate E -plane and H -plane, respectively. Red arrows show the direction of plane wave incidence.

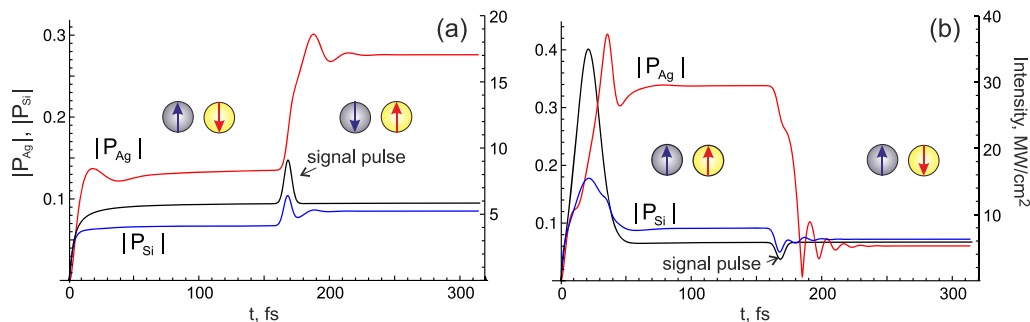


Figure 5. Temporal dependencies of $|P_{Ag}|$ (red), $|P_{Si}|$ (blue) and intensity of the external field (black) when the signal pulse provokes a transition (a) from the back scattering state 1 to the fourth scattering state 2 and (b) from the omnidirectional scattering state 3 to the back scattering state 4. Movies 1 and 2 (available at stacks.iop.org/NJP/14/093005/mmedia), demonstrate the dynamical behavior of the system's scattering pattern, corresponding to (a) and (b), respectively.

for ultrafast all-optical switching. Furthermore, it appears to be a competitive alternative to optical switches based on semiconductor microcavities, as well as plasmonic nanoantennas with nonlinear dielectric and semiconductor loading, whose minimal switching time is of several picoseconds [12, 15, 36].

Apparently, when the external electric field is polarized along the y -axis in the linear regime, one can excite in the dimer a longitudinal dipole mode at $\omega = \omega_0$ or linear quadrupole modes with positive and negative relative phase shifts at $\omega > \omega_0$ and $\omega < \omega_0$, respectively [4, 5]. Consequently, a bistable response of the silver nanoparticle will result in the dipole–quadrupole and quadrupole–quadrupole dynamical transitions of the system's scattering pattern in the manner similar to that described above.

In practice, Si–Ag heterodimers can be obtained through a recently suggested combination of top-down fabrication and template-guided self-assembly [37], which allows the precise and controllable vertical and horizontal positioning of the plasmonic elements relative to dielectric spheres. Atomic force microscopy nanomanipulation is another useful approach for the construction of such hybrid systems [38–40].

4. Conclusions

We have predicted a bistable response of a hybrid nonlinear Si–Ag nanoantenna and revealed that its radiation pattern can be reversed by varying the external intensity. This effect originates from the phase shift between the dipole moments of the nanoparticles, caused by differences in the polarizabilities between Si and Ag nanoparticles, induced by the intrinsic nonlinearity of a silver particle and the different dispersions and sizes of the particles. A characteristic switching time of 40 fs, along with the relatively low required intensity of 6 MW cm^{-2} can be useful for ultrafast logical hybrid nanophotonic–plasmonic devices and circuitry.

Acknowledgments

The authors are indebted to A A Zharov, A E Miroshnichenko and I S Maximov for useful comments, to P A Belov for stimulating discussions and to the Ministry of Education and Science of Russian Federation and the Australian Research Council for a financial support.

References

- [1] Bharadwaj P, Deutsch B and Novotny L 2009 Optical antennas *Adv. Opt. Photon.* **1** 438
- [2] Novotny L and van Hulst N 2011 Antennas for light *Nature Photon.* **5** 83
- [3] Giannini V, Fernández-Domínguez A I, Heck S C and Maier S A 2011 Plasmonic nanoantennas: fundamentals and their use in controlling the radiative properties of nanoemitters *Chem. Rev.* **111** 3888
- [4] Sheikholeslami S, Jun Y-W, Jain P K and Alivisatos A P 2010 Coupling of optical resonances in a compositionally asymmetric plasmonic nanoparticle dimer *Nano Lett.* **10** 2655
- [5] Shegai T, Chen S, Miljković V D, Zengin G, Johansson P and Käll M 2011 A bimetallic nanoantenna for directional colour routing *Nature Commun.* **2** 481
- [6] Kosako T, Kadoya Y and Hofmann H F 2010 Directional control of light by a nanooptical Yagi–Uda antenna *Nature Photon.* **4** 312
- [7] Dorfmueller J, Dregely D, Esslinger M, Khunsin W, Vogelgesang R, Kern K and Giessen H 2011 Near-field dynamics of optical Yagi–Uda nanoantennas *Nano Lett.* **11** 2819
- [8] Huang F and Baumberg J J 2010 Actively tuned plasmons on elastometrically driven Au nanoparticle dimers *Nano Lett.* **10** 1787
- [9] Devilez A, Stout B and Bonod N 2010 Compact metallo-dielectric optical antenna for ultra directional and enhanced radiative emission *ACS Nano* **4** 3390
- [10] Krasnok A E, Miroshnichenko A E, Belov P A and Kivshar Yu S 2011 Huygens optical elements and Yagi–Uda nanoantennas based on dielectric nanoparticles *JETP Lett.* **94** 593
- [11] Chen Y, Lodahl P and Koenderink A F 2010 Dynamically reconfigurable directionality of plasmon-based single photon sources *Phys. Rev. B* **82** 081402
- [12] Berthelot J *et al* 2009 Tuning of an optical dimer nanoantenna by electrically controlling its load impedance *Nano Lett.* **9** 3914
- [13] Chen P-Y and Alù A 2010 Optical nanoantenna arrays loaded with nonlinear materials *Phys. Rev. B* **82** 235405
- [14] Large N, Abb M, Aizpurua J and Muskens O L 2010 Photoconductively loaded plasmonic nanoantenna as building block for ultracompact optical switches *Nano Lett.* **10** 1741
- [15] Abb M, Albella P, Aizpurua J and Muskens O L 2011 All-optical control of a single plasmonic nanoantenna-to hybrid *Nano Lett.* **11** 2457
- [16] Maksymov I S, Miroshnichenko A E and Kivshar Yu S 2012 Actively tunable bistable optical Yagi–Uda nanoantenna *Opt. Express* **20** 8929
- [17] Olivares I, Rojas R and Claro F 1987 Surface modes of a pair of unequal spheres *Phys. Rev. B* **35** 2453
- [18] Gozhenko V V, Grechko L G and Whites K W 2003 Electrodynamics of spatial clusters of spheres: substrate effects *Phys. Rev. B* **68** 125422
- [19] Romero I, Aizpurua J, Bryant G W and García de Abajo F J 2006 Plasmons in nearly touching metallic nanoparticles: singular response in the limit of touching dimers *Opt. Express* **14** 9988
- [20] Johnson P B and Christy R W 1972 Optical constants of the noble metals *Phys. Rev. B* **6** 4370
- [21] Palik E D (ed) 1985 *Handbook of Optical Constants of Solids* (Orlando, FL: Academic)
- [22] Palpant B 2006 Third-order nonlinear optical response of metal nanoparticles *Non-Linear Optical Properties of Matter* ed M G Papadopoulos, A J Sadlej and J Leszczynski (Dordrecht: Springer) pp 461–508
- [23] Rautian S G 1997 Nonlinear saturation spectroscopy of the degenerate electron gas in spherical metallic particles *J. Exp. Theor. Phys.* **85** 451

- [24] Drachev V P, Buin A K, Nakotte H and Shalaev V M 2004 Size dependent $\chi^{(3)}$ for conduction electrons in Ag nanoparticles *Nano Lett.* **4** 1535
- [25] Govyadinov A A, Panasyuk G Y, Schotland J C and Markel V A 2011 Theoretical and numerical investigation of the size-dependent optical effects in metal nanoparticles *Phys. Rev. B* **84** 155461
- [26] Ricard D, Roussignol Ph and Flytzanis Chr 1985 Surface-mediated enhancement of optical phase conjugation in metal colloids *Opt. Lett.* **10** 511
- [27] Uchida K, Kaneko S, Omi S, Hata C, Tanji H, Asahara Y and Ikushima A J 1994 Optical nonlinearities of a high concentration of small metal particles dispersed in glass: copper and silver particles *J. Opt. Soc. Am. B* **11** 1236
- [28] Dinu M, Quochi F and Garcia H 2003 Third-order nonlinearities in silicon at telecom wavelengths *Appl. Phys. Lett.* **82** 2954
- [29] Weber M J 2003 *Handbook of Optical Materials* (Boca Raton, FL: CRC)
- [30] Stratton J A 1941 *Electromagnetic Theory* (New York: McGraw-Hill)
- [31] Wokaun A, Gordon J P and Liao P F 1982 Radiation damping in surface-enhanced Raman scattering *Phys. Rev. Lett.* **48** 957
- [32] Whitham G B 1974 *Linear and Nonlinear Waves* (New York: Wiley)
- [33] Noskov R E, Belov P A and Kivshar Yu S 2012 Subwavelength modulational instability and plasmon oscillons in nanoparticle arrays *Phys. Rev. Lett.* **108** 093901
- [34] Torres-Torres C, Peréa-López N, Reyes-Esqueda J A, Rodríguez-Fernández L, Crespo-Sosa A, Cheang-Wong J C and Oliver A 2010 Ablation and optical third-order nonlinearities in Ag nanoparticles *Int. J. Nanomed.* **5** 925
- [35] Harrison R K and Ben-Yakar A 2010 Role of near-field enhancement in plasmonic laser nanoablation using gold nanorods on a silicon substrate *Opt. Express* **18** 22556
- [36] Menon V M, Deych L I and Lisyansky A A 2010 Towards polaritonic logic circuits *Nature Photon.* **4** 345
- [37] Ahn W, Boriskina S V, Hong Y and Reinhard B M 2012 Photonic-plasmonic mode coupling in on-chip integrated optoplasmonic molecules *ACS Nano* **6** 951
- [38] Schietinger S, Barth M, Aichele T and Benson O 2009 Plasmon-enhanced single photon emission from a nanoassembled metal-diamond hybrid structure at room temperature *Nano Lett.* **9** 1694
- [39] Ratchford D, Shafiei F, Kim S, Gray S K and Li X 2011 Manipulating coupling between a single semiconductor quantum dot and single gold nanoparticle *Nano Lett.* **11** 1049
- [40] Benson O 2011 Assembly of hybrid photonic architectures from nanophotonic constituents *Nature* **480** 193